Photoisomerization of diphenylbutadiene in low-viscosity nonpolar solvents: Experimental manifestations of multidimensional Kramers behavior and cluster effects

Ch. Gehrke, J. Schroeder, D. Schwarzer, J. Troe, and F. Voß
Institut für Physikalische Chemie der Universität, Universität Göttingen, Tammannstr. 6, D-3400 Göttingen, West Germany

(Received 28 July 1989; accepted 15 November 1989)

The photoisomerization of diphenylbutadiene was studied by picosecond absorption spectroscopy over wide pressure and temperature ranges in liquid and supercritical alkanes, CO_2, SF_6, and He. The reaction shows typical features of a thermal unimolecular reaction on the S_1 potential energy surface. The rate can be expressed by a combination of standard unimolecular rate theory and Kramers–Smoluchowski theory. However, multidimensional behavior manifests itself in the transition to the gas phase low pressure range as well as to the high density Kramers–Smoluchowski range: in the former case, the low pressure limit of a unimolecular reaction of the polyatomic molecule is approached; in the latter case, the effective imaginary barrier frequency shows a marked apparent temperature dependence. The experiments also suggest contributions of reactant–solvent cluster interactions, which modify the barrier height even in nonpolar solvents.

I. INTRODUCTION

Reactions in dense media are governed by complex reactant–solvent interactions.

(i) The reactants can be activated or deactivated by binary collisions or cooperative couplings with the solvent.

(ii) The dynamics can be influenced by viscous or viscoelastic forces of the medium.

(iii) The potential energy of the reactants can be modified by reactant–solvent interactions, either in clusters or in densely packed solvent cages.

These different "effects" in general are difficult to separate. Nevertheless under special experimental conditions one of these aspects of the reactant–solvent interactions may dominate. The present work intends to describe the creation of such conditions for the well-behaved unimolecular isomerization of electronically excited diphenylbutadiene (DPB), i.e., it addresses a typical barrier crossing problem.

The following points distinguish this reaction from less well-studied cases.

(i) It was investigated earlier in supersonic expansions under isolated molecule conditions.[1–4] An analysis of the results was possible by an RRKM fit with a minimum number of adjustable parameters.[5] In this way the high pressure rate constant k_∞ of the thermal unimolecular reaction can be modeled, assuming complete absence of reactant–solvent interactions.

(ii) The calculated value of k_∞ is close to results from measurements in compressed gases and low-viscosity nonpolar solvents.[6–9] These observations, therefore, suggest only very minor solvent shifts of the reaction barrier.

(iii) Preliminary measurements in compressed low-viscosity solvents[7,10] indicate a Kramers–Smoluchowski type decrease of the rate coefficient with increasing viscosity. Deviations from this behavior were observed at viscosities greater than 1 cP in compressed liquid *n*-octane.[6]

(iv) In search of the so-called "Kramers–turnover" of the reaction rate, measurements of the temperature dependence in liquid ethane and propane revealed an increasingly steeper rise of the rate constant with decreasing viscosity.[8]

The DPB system appears to behave remarkably different from the analogous trans-stilbene system, for which the measured rate constants in high pressure gases and low-viscosity liquids by far exceed the modeled k_∞ value (see, e.g., Refs. 11–25). The first aim of the present work, therefore, was a careful investigation of the high pressure gas phase and low-viscosity liquid limiting rate constant for DPB. Even if the preliminary measurements suggested agreement with the modeled k_∞, there may, nevertheless, be specific solvent effects present, which can only be identified by comparing pressure dependent experiments in different solvents. Our present observations of this type, like those for stilbene, are interpreted as "*cluster effects*." Although the experimental evidence for this effect appears convincing, separate experiments in isolated DPB-solvent clusters still have to confirm this hypothesis (for a discussion of alternative explanations, see, e.g., Refs. 24 and 25).

Apart from the study of cluster effects, we investigate the role of transport contributions to the reaction rate in low-viscosity nonpolar solvents. By varying the viscosity via increasing the pressure in a single solvent, the validity of a Kramers–Smoluchowski description of the reaction can be examined much better than by using a series of different solvents at ambient pressure. We have followed this philosophy successfully in a large number of earlier studies in our laboratory (see summaries in Refs. 10 and 26). In the present work we observe that for low-viscosity solvents the reaction rate is correctly described by a *Kramers–Smoluchowski solvent friction dependence*, i.e.,

$$k \propto k_\infty / \beta, \tag{1}$$

where β is the friction coefficient. A frequently discussed relationship of the type

 0021-9606/90/084805-12$03.00

$$k \propto k_\infty / \eta^a, \quad a < 1 \tag{2}$$

does not apply in the experiments discussed here.

A further test of the Kramers formalism can be performed by investigating the temperature dependence of the rate coefficient k at constant friction in the Kramers–Smoluchowski range, where Eq. (1) applies. We find a much stronger temperature dependence of k than given by the contribution from the modeled k_∞ in Eq. (1). We interpret this observation as an experimental manifestation of *multidimensional barrier effects*. We attribute the observed temperature dependence to the specific properties of the multidimensional potential energy surface in the barrier region. We give a simple model representation and relate this interpretation to our recent quantum-chemical calculations of the corresponding barrier in trans-stilbene.[27]

Multidimensional effects in barrier crossing problems have found attention in a number of recent publications. There is the "trivial" multidimensional behavior in the weak-damping regime, where standard unimolecular rate theory is approached.[26,28–30] For quite a while, this has been overlooked in discussions of one-dimensional "Kramers turnovers," it is, however, generally accepted now.[31] Multidimensional effects in the strong-damping regime[32–35] may become apparent in the case of anisotropic friction.[36,37] The topology of the barrier region also can play a role.[38–40] The present work suggests an experimental manifestation of the latter effects in form of the temperature dependence of the rate coefficient. Deviations from an inverted parabolic potential in the reaction coordinate also[40,41] lead to deviations of the temperature dependence from that given by k_∞ in Eq. (1). However, the effects observed in the present work are too large to be explained in this way. Instead, we attribute our results to a dependence of the imaginary barrier frequency in the reaction coordinate on the excitation of coordinates "perpendicular" to the reaction coordinate. On the basis of our quantum-chemical calculations for the stilbene system,[27] we demonstrate how large effects can be caused by this property of the potential energy surface.

II. EXPERIMENTAL TECHNIQUE

Rate coefficients of electronically excited E,E-1,4-diphenyl-butadiene(1.3) (trans-DPB) were determined from the decay of the transient absorption at 616 nm after exciting the sample at 308 nm employing a picosecond pump-probe technique. The picosecond pulses in our system[19] were generated by a Coherent 599 dye laser synchronously pumped at 514 nm by an Ar^+ laser (Coherent Innova 10 tube). The output pulses of approximately 2.5 psec duration at 616 nm were amplified in a three stage dye amplifier chain pumped by the frequency doubled output pulses from a Quanta Ray DCR1-A Nd-YAG laser at a repetition rate of 10 Hz. The amplified picosecond pulses, which showed the same autocorrelation trace as the input pulses, were frequency doubled in a KD*P crystal of 1 mm thickness and subsequently passed twice through the channel of a properly synchronized XeCl-exciplex laser (Lambda Physik EMG 150) to amplify the UV-picosecond pulses at 308 nm. The pulses were then split and recombined in a standard pump-probe interferometer arrangement. The pump energy reaching the sample cell was about 0.3 mJ at 308 nm, and the probe energy of the 616 nm pulse was about 0.05 mJ. Pulse energies were measured in front of and behind the sample cell with photodiodes, whose output was integrated, digitized, and fed into a computer. The plane of polarization of the probe beam could be varied by means of a zeroth-order half-wave plate to study effects of overall rotational relaxation on the transient absorption signals. Signals from the pump pulse photodiode were discriminated, eliminating pulses with energies differing by more than 10% from a nominal value. Blank signals were recorded in a similar way. Samples of 200 mm thickness were used in high pressure gas phase experiments, and of 20 mm or 1.8 mm in liquid phase measurements. The temperature of the cell was controlled to one degree accuracy in gas phase experiments. Special care was taken to eliminate photocondensation of photoproducts on the inner surface of the cell windows, which were kept at a slightly higher temperature than the cell body. More details of our experimental setup can be found in Ref. 19. Solvents, gases, and trans DPB were of the highest commercially available purity and used without further purification.

III. EXPERIMENTAL RESULTS

The transient absorption of trans DPB at 616 nm, which was measured in a "magic" angle arrangement[42] of the planes of polarization of pump and probe pulses, first shows a rapid increase with a rise time of 3–4 psec followed by a slower decay obeying first-order kinetics with rate coefficients k_{exp}. The fast rise time may be compared with a cross-correlation width of pump and probe pulses of 3.5 psec and reflects the time resolution of our picosecond system. This transient absorption was assigned to the lowest excited singlet state of trans DPB in solution.[43] Figure 1 shows an absorption-time profile with the associated blank signal. From the signal decay we obtained the isomerization rate coeffi-

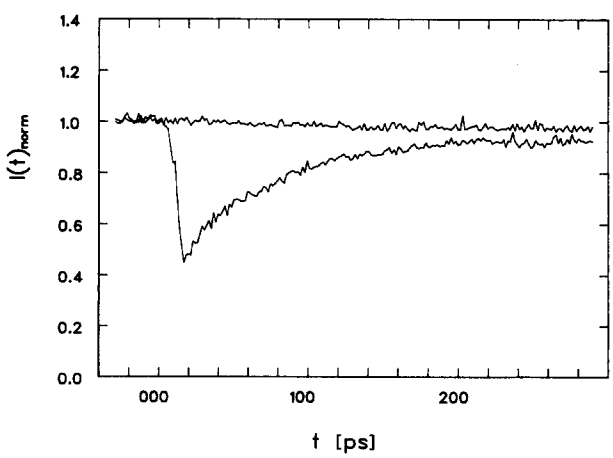

FIG. 1. Photoisomerization of DPB in ethane ($p = 298$ bar, $T = 354$ K). Plot of normalized transmitted intensity at 616 nm versus delay time. Upper trace: without UV excitation; lower trace: with UV excitation. Each trace consists of 250 discrete data points. (The long lived absorption is excitation intensity dependent and tentatively assigned to the DPB^+ cation produced by multiphoton ionization.[44])

TABLE I. Experimental photoisomerization rate coefficients k of diphenylbutadiene in gases and supercritical fluids.

p/MPa	T/K	$[M]/10^{-2}$ mol cm^{-3}	η/cP*	$D/10^{-4}$ cm^2 s^{-1}	k/10^9 s^{-1}
Ethane					
2.95	388	0.103[a]	0.013[a]	46.4[g]	50
12.1	336	1.02	0.036	4.1	13.7
26.6	340	1.28	0.055	3.3[h]	10.0
27.5	343	1.28	0.056	3.3	10.0
29.2	337	1.32	0.060	3.2	10.0
130	337	1.78[b]		1.5	5.5
290	337	2.04		0.85	3.5
26.8	365	1.20[a]	0.049	3.8	15.9
33.0	370	1.24	0.054	3.7	16.8
62.0	371	1.44	0.071	2.7	14.1
90.0	372	1.52	0.085	2.4	13.0
270	372	1.94[b]		1.2	7.0
24.0	306	1.41[a]	0.067	2.6	4.2
21.4	316	1.34	0.061	2.9	5.7
25.0	325	1.33	0.060	3.0	6.7
28.3	348	1.28	0.056	3.4	14.0
29.6	354	1.26	0.053	3.5	15.0
30.0	356	1.26	0.054	3.5	12.9
34.5	382	1.21	0.052	3.9	24
37.5	399	1.17	0.048	4.2	31
38.3	405	1.15	0.047	4.3	31
40.9	421	1.14	0.047	4.5	45
Propane					
13.0	393	0.862[a]	0.052[a]	2.7[i]	19.6
17.0	386	0.945	0.061	2.3	16.4
51.0	393	1.12	0.10	1.4	16.3
89.0	393	1.22	0.13	1.2	15.1
220	393	1.38[c]	0.21[d]	0.86	12.2
330	393	1.45	0.35	0.53	8.9
450	393	1.50	0.42	0.46	7.2
n-Butane					
0.34	407	0.0108[a]	0.010[a]	225[j]	40
CO_2					
5.3	384	0.187[e]	0.019[e]	28.0[g]	50
21.8	332	1.69	0.064	2.2[i]	21.3
51.5	350	2.01	0.089	1.8	24.5
145	350	2.51	0.155	1.11	23.9
235	350	2.75	0.24	0.75	21.5
379	350	3.03	0.38	0.50	18.7
SF_6					
3.32	364	0.141[f]		10.7[g]	27
3.32	388	0.132		12.1	32
Helium					
29.2	429	0.819[f]		62[j]	40

[a] Reference 71.
[b] Extrapolated from Ref. 71 following Ref. 62.
[c] Extrapolated from Ref. 72 following Ref. 62.
[d] Extrapolated from Ref. 73 following Ref. 62.
[e] Reference 74.
[f] Calculated from Pitzer's correlation following Ref. 62.
[g] Reference 75.
[h] Extrapolated from Ref. 46.
[i] Extrapolated from Ref. 76 via density dependence of $\eta \cdot D$.
[j] Gas kinetic value using Lennard-Jones collision integrals.
*1 cP = 10^{-3} Pa sec.

cient by subtracting the radiative rate coefficient[6] $k_r = [1.4 \cdot f(n^2) + 0.43] \cdot 10^9$ sec^{-1} from the measured first-order rate coefficient, where n is the refractive index of the solvent and $f(n^2) = (n^2 - 1)/(n^2 + 2)$. Here we assume that the nonradiative decay of the observed excited singlet state of trans DPB is dominated by rotation about one of the two double bonds and that the subsequent internal conversion to the electronic ground state is a very rapid process. The resulting values of $k = k_{exp} - k_r$ are listed in Table I for gaseous and supercritical fluid solvents at various temperatures, and in Table II for liquid solvents for room temperature (298 K).

The rate coefficients k measured in the three linear alkane solvents ethane, propane, and *n*-butane are plotted versus the inverse of the corresponding self-diffusion coefficient D^{-1} of the solvent in Fig. 2 on a double logarithmic scale. As discussed earlier,[10,19,45] D^{-1} can be taken as a parameter related to an effective collision frequency scale over the entire density range, extending from the dilute gas to the compressed liquid phase. Diffusion coefficients for liquid and dense fluid solvents were taken directly or extrapolated from experimental self diffusion coefficients or viscosity data (see footnotes of Tables I and II). For the low density gas phase, it was sufficient to calculate the gas kinetic diffusion coefficients using pVT data and Lennard-Jones collision integrals.[47]

The rate coefficient of photoisomerization decreases by more than two orders of magnitude when the pressure is

TABLE II. Experimental photoisomerization rate coefficients k of diphenylbutadiene in liquid solvents.

p/MPa	T/K	$[M]/10^{-2}$ mol cm^{-3}	η/cP*	$D/10^{-4}$ cm^2 s^{-1}	k/10^9 s^{-1}
Ethane					
3.9	295	1.115[a]	0.039[a]	3.7[h]	6.1
10.0		1.30	0.055	3.0	4.1
21.2	298	1.41	0.068	2.6	3.8
22.5	295	1.44	0.073	2.4	3.0
51.0		1.59	0.093	1.8	2.3
205		1.99[b]	0.265[c]	0.89	1.2
310		2.10	0.34	0.68	0.80
420		2.19	0.44	0.54	0.71
620		2.31	0.60	0.38	0.48
Propane					
1.50	298	1.12[a]	0.098[a]	1.22[i]	3.41
2.40		1.13	0.099	1.21	3.30
3.30		1.14	0.102	1.20	3.14
17.0		1.19	0.124	1.10	2.36
70.0		1.33	0.189	0.79	1.66
150		1.42[d]	0.31[e]	0.52	1.10
300		1.55	0.53	0.34	0.75
390		1.60	0.69	0.28	0.58
500		1.66	0.84	0.24	0.60
n-Butane					
0.24	298	0.986[a]	0.157[a]	0.70[i]	4.2
3.0		0.99	0.167	0.66	4.71
50.0		1.08	0.251	0.44	2.94
80.0		1.12	0.301	0.43	2.45
128		1.21[b]	0.33[e]	0.39	2.16
310		1.27	0.83	0.18	1.12
378		1.29	1.00	0.16	1.02
390		1.30	1.04	0.15	0.99
416		1.31	1.10	0.15	0.91
440		1.32	1.18	0.14	0.82
470		1.34	1.30	0.13	0.79
n-Pentane					
0.10	298	0.86[f]	0.228[g]	0.56[i]	1.50
n-Decane					
0.10	298	0.51[f]	0.897[g]	0.14[i]	0.56

[a] Reference 71.
[b] Estimated following Ref. 62.
[c] Reference 77.
[d] Reference 72.
[e] Reference 73.
[f] Reference 79.
[g] Reference 78.
[h] Reference 46.
[i] Extrapolated from Ref. 76 via density dependence of ηD.
[j] Reference 80.
*1 cP = 10^{-3} Pa sec.

raised from about 0.3 MPa in the gas phase to 62 MPa in the liquid phase. In the liquid, the rate coefficients are proportional to the self-diffusion coefficient in all three solvents. At a constant diffusion coefficient, their values increase roughly by a factor of 2 from ethane to propane, and from propane to *n*-butane, respectively. The gas phase measurements had to be performed at a higher temperature to obtain a sufficient vapor pressure of DPB. They were converted to the temperature of the liquid phase experiments using the known temperature coefficient of k_∞, see below. A similar procedure was used in our earlier studies of trans-stilbene photoisomerization.[10,19,45] Our rate coefficients in other nonpolar solvents are plotted in Fig. 3 together with data from Velsko and Fleming.[6] The measurements in liquid ethane and *n*-butane (Fig. 2) are indicated by the two dashed lines. The rate coefficients measured in the four higher alkanes at 1 bar pressure are all quite close to those measured in propane. As in Fig. 2, the rate coefficients measured in gaseous helium and in supercritical CO_2 and SF_6 were scaled down to room temperature.

In our earlier work on trans-stilbene we have discussed possible connections between density dependent solvent shifts of the effective barriers for photoisomerization and of the UV-absorption spectra.[11,45] In a similar way we have now measured the pressure dependent shift of the UV-absorption maximum of trans-DPB near 325 nm, with respect to its position in the low pressure vapor.[49] The shape of the spectrum remains constant with increasing pressure, and the shifts are plotted in Fig. 4 as a function of $f(n^2)$, which is a measure of solvent polarity, because the solvents possess no permanent dipole moment. Whereas one obtains the expected linear relationship between polarity and spectral shift in the regime of "normal" liquidlike densities [$f(n^2) > 0.17$], it is interesting to note the deviation from this linear correlation toward lower densities in the gas and low pressure liquid phase in ethane, CO_2, and SF_6. This transition of the density dependence of the solvatochromic shift from gaslike to liquidlike densities has also been observed in other systems.[50]

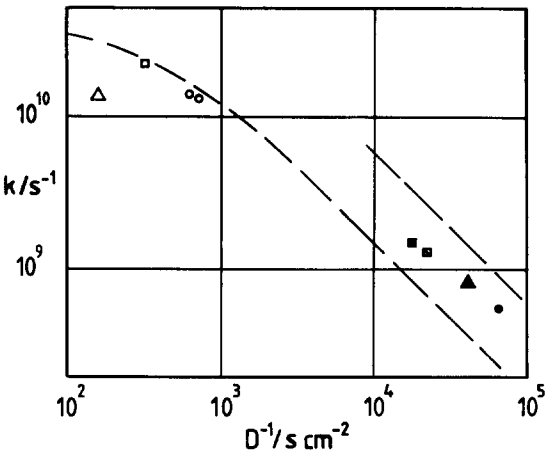

FIG. 3. Photoisomerization rate coefficients k at room temperature in helium (△), CO_2 (□), SF_6 (○), *n*-pentane (■), and *n*-decane (●) from this work, and in *n*-hexane (⊠) and *n*-octane (▲) from Ref. 5. The dashed lines indicate the rate coefficients measured in ethane (left) and *n*-butane (right) from Fig. 2.

In addition to our experiments on the pressure dependence of the rate coefficient k, we also investigated its temperature dependence in supercritical ethane, propane, and CO_2. The results complement earlier measurements of the temperature coefficients of k for DPB by Courtney and Fleming in liquid ethane and propane in the low temperature liquid.[8] Figure 5 shows three isotherms of k vs D^{-1} in liquid and supercritical ethane, Fig. 6 isotherms for liquid and supercritical propane, and supercritical CO_2. The dependence of k on D becomes weaker with increasing temperature in all three cases, whereas the rate coefficients show the expected increase with temperature. We also performed a series of experiments in supercritical ethane to study the temperature dependence in more detail, where—by applying the appropriate pressure—we kept the solvent self-diffusion coefficient in the range $2 \leqslant D \leqslant 4 \cdot 10^{-4}$ cm^2 s^{-1}, i.e., corresponding

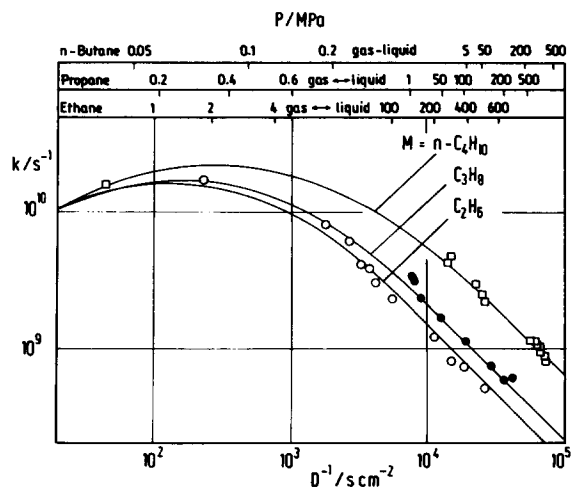

FIG. 2. Photoisomerization rate coefficients k for DPB in compressed ethane (○), propane (●), and *n*-butane (□) at room temperature versus the inverse of the self-diffusion coefficient D of these solvents. (Solid lines from two parameter fits, see the text, with the parameters $E_{0,cl} = 850$ cm^{-1} and ω_B is $5.0 \cdot 10^{11}$ sec^{-1} for ethane, $6.5 \cdot 10^{11}$ sec^{-1} for propane, and $2.0 \cdot 10^{12}$ sec^{-1} for *n*-butane.)

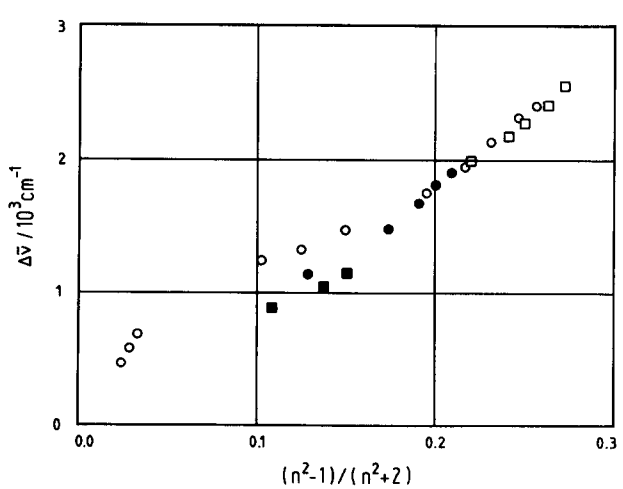

FIG. 4. Shift of the peak of UV absorption spectrum of DPB in compressed ethane (○), propane (●), CO_2 (□), and SF_6 (■) with respect to the low pressure vapor spectrum versus the solvent polarizability parameter (n = refractive index of the solvent).

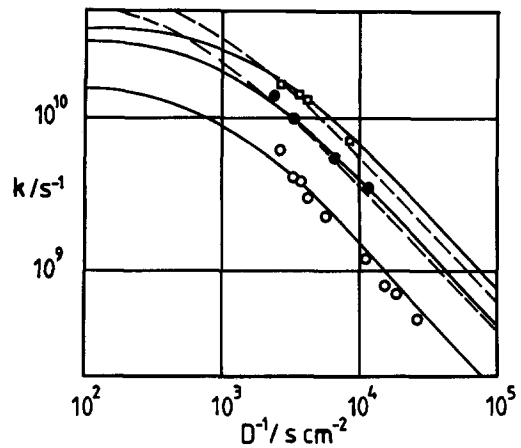

FIG. 5. Photoisomerization rate coefficients k of DPB in ethane at three different temperatures: (O) 295 K, (●) 337 K, and (□) 370 K. Dashed curves: model fit (see text) with constant $\omega_B = 5\cdot10^{11}$ sec^{-1} and temperature dependent $E_{0,cl}$ [$E_{0,cl}$(295 K) = 850 cm^{-1}, $E_{0,cl}$(337 K) = 700 cm^{-1}, and $E_{0,cl}$(370 K) = 650 cm^{-1}]. Solid curves: model fit (see text) with constant $E_{0,cl} = 850$ cm^{-1} and temperature dependent ω_B [ω_B(295 K) = $5.0\cdot10^{11}$ sec^{-1}, ω_B(337 K) = $1.1\cdot10^{12}$ sec^{-1}, and ω_B(370 K) = $1.5\cdot10^{12}$ sec^{-1}].

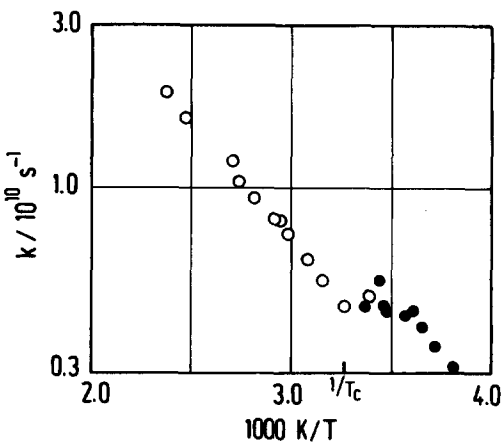

FIG. 7. Temperature dependence of the rate coefficient in ethane at $2.0 \leqslant D \leqslant 4.0\cdot10^{-4}$ cm^2 sec^{-1}; (O) this work; (●) rate coefficients from Ref. 8.

to values typical for a low-viscosity liquid. The results are shown in Fig. 7, where we plot k versus the inverse temperature, together with the rate coefficients obtained in liquid ethane at low temperatures by Fleming and Courtney.[8] Evidently, there is a change of the apparent activation energy in the vicinity of the critical temperature of ethane, $T_c = 305.4$ K.

IV. DISCUSSION

A. Falloff curves of the thermal unimolecular isomerization

At first, we compare our experimental data, obtained at the lowest densities, with calculations for the thermal unimolecular reaction. The high precision of the lifetime measurements for jet-cooled, isolated trans-DPB molecules[1,2] allowed the construction of an optimized RRKM fit to the specific rate constants $k(E)$ of the reaction.[5] The threshold energy E_0 and an average activated complex frequency scaling factor could be fixed. After thermal averaging of $k(E)$ over an equilibrium population $f(E)$, this analysis with good reliability leads to the limiting "high pressure" gas phase rate coefficient k_∞:

$$k_\infty = \int_{E_0}^{\infty} k(E)f(E)dE. \tag{3}$$

In the analogous procedure for simple bond fission reactions, the rotational dependence of $k(E,J)$ has to be properly taken into account since it has a large effect.[51] The present analysis of a rigid activated complex isomerization has neglected this aspect. While the $k(E)$ measured in supersonic jets correspond to very low J values ($\langle J\rangle \approx 1$),[5] the k_∞ measured near room temperature include contributions from higher values of J. This is taken into account by multiplying Eq. (3) by a factor $Q^{\ddagger}_{rot}/Q_{rot} \approx I^{\ddagger}/I$ (Q_{rot} denotes rotational partition function, I is the moment of inertia, which typically will be between 1 and 2. More information on this factor would require knowledge about the activated complex structure. Considering this lack of information, we estimate the uncertainty of the modeled limiting rate coefficient,[5]

$$k_\infty = 6.9\cdot10^{11}\cdot\exp(-11.5 \text{ kJ mol}^{-1}/RT)\text{sec}^{-1},$$
$$(260 \text{ K} \leqslant T \leqslant 410 \text{ K}) \tag{4}$$

to be about a factor of 2.

Neglecting weak collision effects, standard unimolecular rate theory expresses the limiting low pressure rate coefficient k_0 as [53,54]

$$k_0 = \beta_c Z_{LJ}\cdot[M]\int_{E_0}^{\infty} f(E)dE, \tag{5}$$

where $[M]$ denotes solvent concentration. The evaluation of this equation requires a complete set of vibrational frequencies for trans DPB, which was taken from Ref. 52. Neglecting correction factors for rotation and anharmonicity, $F_{rot} = I^{\ddagger}/I \approx 1$ and $F_{anh} \approx 1$, using $\beta_c \approx 1$, and estimating Len-

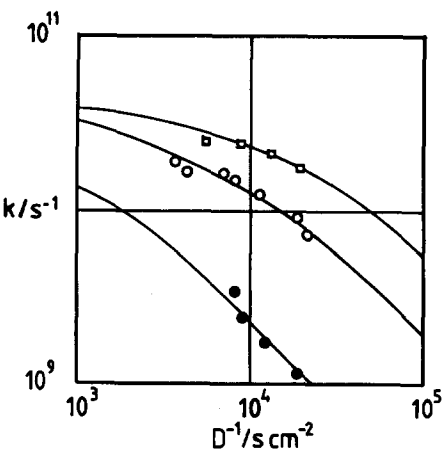

FIG. 6. Photoisomerization rate coefficients of DPB in propane at 298 K (●) and 390 K (O), and CO_2 at 350 K (□). Solid lines: model fits (see text) with $E_{0,cl} = 850$ cm^{-1}, ω_B(298 K) = $6.5\cdot10^{11}$ sec^{-1}, and ω_B(390 K) = $2.5\cdot10^{12}$ sec^{-1} for propane, and $E_{0,cl} = 900$ cm^{-1} and ω_B(350 K) = $3\cdot10^{13}$ sec^{-1} for CO_2.

nard-Jones collision frequencies Z_{LJ} in Eq. (5) for ethane leads to

$$k_0 \approx 2.5 \cdot 10^{13} \cdot [M] \cdot \sqrt{T/\mathrm{K}} \cdot \exp(-1.40 \text{ kJ mol}^{-1}/RT)\,\mathrm{cm^3\,mol^{-1}\,s^{-1}}. \quad (6)$$

Equations (4) and (6) then yield falloff curves for the photoisomerization rate coefficients k under thermalized conditions at various temperatures. Broadening effects[54] of the transition of k from k_0 to k_∞ here are only of minor importance: Our detailed RRKM modeling[5] has led to broadening factors $F_c = 0.82$ at 300 K and $F_c = 0.92$ at 400 K, such that $k/k_\infty \approx F_c/2$ at the center of the falloff curve where $k_0/k_\infty = 1$. (One should note the anomalous temperature dependence of F_c.) At sufficiently low pressures in thermal gases, however, k would not approach k_0, since thermalization after photoexcitation is not achieved sufficiently rapidly. Instead, one would observe a rate coefficient that depends on the wavelength of excitation, corresponding to the yield of a photochemical activation system.[55] Since here we are interested in high pressure phenomena, we neglect these effects and use only the Lindemann–Hinshelwood expression

$$1/k \approx 1/k_0 + 1/k_\infty . \quad (7)$$

The fact that the measured k is close to the calculated value of k_∞ represents one of the manifestations of the multidimensional character of the problem. If one-dimensional instead of multidimensional unimolecular rate theory would apply, k_0 should be expected to attain a value of the order of $k_0 \approx 10^{14} \cdot [M] \cdot \exp(-11.5 \text{ kJ mol}^{-1}/RT)\ \mathrm{cm^3\,mol^{-1}\,sec^{-1}}$ instead of that given by Eq. (6). At $[M] \approx 10^{-4}$ mol/cm^3 and $T = 407$ K, its value would be equal to $k_0 \approx 3 \cdot 10^8$ sec^{-1}, which is two orders of magnitude below the rate coefficient measured under these conditions (see Table I). This "trivial" multidimensional behavior in the weak-damping regime is responsible for the higher rate.

B. Cluster effects in the very low friction range

In contrast to the trans-stilbene system, where the modeled k_∞ in high pressure gases differs from the measured k_∞ by a factor of 50[23], in trans-DPB the measured value is only about twice as large as the one derived from Eq. (3). This discrepancy is still within the uncertainty of the analysis, so that a difference between the measured k and the calculated k_∞ in high pressure gases cannot be deduced from measurements within a single solvent. In terms of a combined unimolecular reaction–Kramers model, with

$$\frac{1}{k} \approx \frac{1}{k_0} + \frac{1}{k_\infty} + \frac{1}{k_{\mathrm{diff}}}, \quad (8)$$

however, there should be no dependence of $k \approx k_\infty$ on the nature of the solvent, apart from the onset of the transition of k from k_∞ to k_{diff}. We have tested this conclusion by comparing it with our results in different gaseous supercritical solvents at densities, where diffussion effects are not yet important, i.e., at viscosities where one may still use Eq. (7) instead of Eq. (8). Figure 8 shows falloff curves calculated from Eqs. (4), (6), and (7) for some temperatures together with the corresponding rate coefficients. There is a systematic deviation of all measured k's toward values that are higher than the calculated k_∞. These deviations amount to a factor of about 2.5 for CO_2, ethane, and n-butane, 1.8 for SF_6, and 1.5 for helium, respectively. (The diffusion coefficients for the different solvents in Fig. 8 were scaled according to the respective solvent molar mass and Lennard-Jones cross section to compare the measured rate coefficients with a single set of temperature dependent falloff curves.)

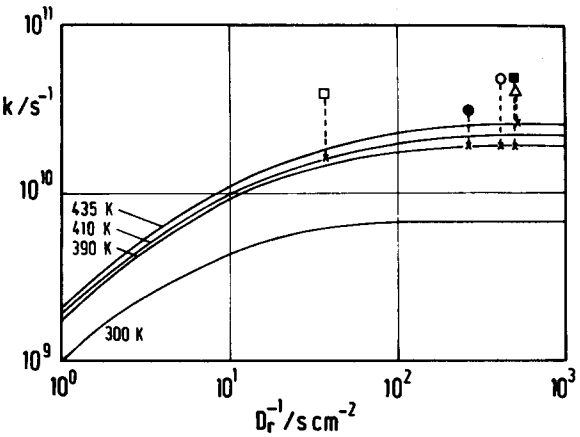

FIG. 8. Falloff curves calculated from Eqs. (4), (6), and (7) for temperatures of the experiments and 300 K (lowest curve) using the threshold energy $E_{0,\mathrm{free}}$ for the isolated DPB molecule (see text, measurements in n-butane at 407 K (□), SF_6 at 388 K (●), ethane at 388 K (○), CO_2 at 384 K (■), and helium at 429 K (△). Reduced diffusion coefficients, see text, are employed such that falloff curves and measurements in different solvent gases can be compared in a single plot.

The solvent dependent discrepancies between the prediction of the simple falloff model and the experiment suggest that specific solute–solvent interactions can accelerate the reaction even at moderate gas pressures. We attribute this phenomenon to a solvent shift of the reaction threshold energy E_0 caused by cluster formation between trans-DPB and solvent molecules M prior to excitation.[10] Leaving the activated complex frequencies unchanged and estimating a value for the cluster equilibrium constant of the order of $K_{\mathrm{cl}} \approx 50 \cdot \mathrm{dm^3\,mol^{-1}}$ for all nonpolar solvents, the experimental points can be fitted by assuming a solvent shift δE of the reaction barrier according to

$$E_{0,\mathrm{cl}} \approx E_{0,\mathrm{free}} - \delta E. \quad (9)$$

The limiting values of the rate coefficient for photoisomerization of trans-DPB in the cluster, $k_{\infty,\mathrm{cl}}$ and $k_{0,\mathrm{cl}}$, are then represented by Eqs. (4) and (6) with modified E_0; those for the free molecule, $k_{\infty,\mathrm{free}}$ and $k_{0,\mathrm{free}}$ are calculated from Eqs. (4) and (6). Assuming only 1–1-solute–solvent complexes, our simplified cluster model then gives the overall values of k_∞ and k_0 by

$$k_0 \approx k_{0,\mathrm{free}}(1 - f_{\mathrm{cl}}) + k_{0,\mathrm{cl}} f_{\mathrm{cl}},$$
$$k_\infty \approx k_{\infty,\mathrm{free}}(1 - f_{\mathrm{cl}}) + k_{\infty,\mathrm{cl}} f_{\mathrm{cl}}, \quad (10)$$

where the fraction of clustered solute molecules is given by

$$f_{\mathrm{cl}} = K_{\mathrm{cl}} \cdot [M]/(1 + K_{\mathrm{cl}} \cdot [M]). \quad (11)$$

Equation (10) implies that—in a certain density range determined by the value of the equilibrium constant—the ex-

perimental decay curves should consist of two exponentially decaying components resulting from free and complexed molecules. We did not observe such behavior under our experimental conditions. The reason could be either that over the entire investigated density range virtually all DPB molecules are complexed, or that our model with just two types of species is too crude and a distribution of differently clustered molecules is present. At present, we cannot rule out this latter possibility, but our spectral solvent shift data suggest that the first alternative gives the more likely explanation. The density range, in which complex formation occurs, probably corresponds to the region of the steeper slope in the plot of spectral shift versus polarizability in ethane in Fig. 4. The densities here are even one order of magnitude smaller than in our time-resolved experiments. This also confirms our estimate of the cluster equilibrium constant.

Applying our simple model as described to the low density rate coefficients of DPB photoisomerization, we obtain the following values for the energy barrier $E_{0,\mathrm{cl}}$ in the clustered molecule: $E_{0,\mathrm{cl}}$ (ethane, *n*-butane) = 10.2 kJ/mol (850 cm^{-1}), $E_{0,\mathrm{cl}}(CO_2)$ = 10.8 kJ/mol (900 cm^{-1}), and $E_{0,\mathrm{cl}}(SF_6,\mathrm{He})$ = 11.4 kJ/mol (950 cm^{-1}). The barrier in the isolated molecule was determined from the RRKM fit to measurements of $k(E)$ in supersonic jet expansions: $E_{0,\mathrm{free}}$ = 13.2 kJ/mol (1100 cm^{-1}).[5]

The order of magnitude of the equilibrium constant does not seem unreasonable in comparison with the value we obtained for cluster formation in the iodine system,[56] which also suggests that clusters play an important role at pressures below those applied in the present work. It would be desirable to test these ideas experimentally by preparing DPB-solvent clusters in a supersonic jet. Measurements of energy specific rate coefficients $k(E)$ under such conditions should exhibit a lowering of the reaction barrier in the cluster with respect to the isolated molecule. Such experiments are underway in our laboratory. Their RRKM analysis may provide a cross-check for the δE values derived here.

The RRKM analysis of energy specific rate coefficients $k(E)$ for the isolated molecule[5] assumes complete intramolecular vibrational energy relaxation (IVR). This assumption is in agreement with the observation that there is no evidence for mode selectivity of DPB photoisomerization[1] that would indicate incomplete IVR. A comparison of the energy dependence of $k(E)$ with the dependence of the canonical rate coefficients in low-viscosity ethane on average vibrational energy, however, has led to the proposition[57] that IVR from the optical mode to the torsional mode is not as effective in the isolated molecule as in solution phase. This slow IVR could explain the increase of the experimental solution phase rate coefficients over the thermally averaged rates obtained in Ref. 5.

A recent study of the deuterium isotope effect in trans-stilbene photoisomerization[58] also reveals inconsistencies with previous RRKM calculations[23,59] concerning the ordering of rate coefficients for deuterated and nondeuterated species. These results are also interpreted as being a result of incomplete, though extensive, IVR in this molecule. A theoretical model incorporating limited IVR into an RRKM-like analysis was developed[60] that qualitatively describes the experimental observations. In this model it is argued that the onset of the experimentally observed $k(E)$ in the isolated molecule is dominated by the onset of IVR and, consequently, does not give the "real" barrier height E_0, which may be lower than the value deduced from a standard RRKM analysis.

However, our MNDO calculations of the activated complex properties in stilbene[27] have revealed a particularly complicated structure, which may lead to an unexpected ordering of rate coefficients for deuterated and nondeuterated molecules. These complications have not been considered in the analysis of Refs. 58–60. Therefore it is difficult to decide on the basis of the experimental and theoretical data presently available, whether this interpretation is valid for the photoisomerization of DPB. The observation that the rates in the range, where $k \approx k_\infty$, depend on the specific carrier gas used, in our view also supports the hypothesis of cluster contributions. At present there exists no undisputed evidence showing that the increase of IVR rates with density exhibits specific solvent effects.

C. Cluster effects in the Kramers–Smoluchowski range

The transition to a transport-controlled reaction, to a first approximation, is expressed by the Kramers–Smoluchowski equation

$$k_{\mathrm{diff}} \approx (\omega_B/\beta)k_\infty \tag{12}$$

with k_∞ from Eq. (10), the imaginary "barrier frequency" ω_B, and the friction coefficient β. The *a priori* identification of the barrier frequency on the basis of known molecular parameters still appears equally difficult as that of a reactant frequency becoming the "reaction coordinate." For molecules of this size, there is presently no possibility for a reliable prediction or even an interpretation of these parameters. Therefore we consider activated complex frequency scaling parameters [in the RRKM fit of $k(E)$] and imaginary barrier frequencies as fit parameters. On the other hand, the friction coefficient β for rotation of the phenyl group can be estimated by the relationship[61]

$$\beta \approx c_1 \eta \sigma_2 r^2 / I_{\mathrm{Ph}}, \tag{13}$$

where η denotes solvent viscosity, $\sigma_2 = 0.37$ nm represents the estimated Lennard-Jones radius of the phenyl group,[62] the radius of gyration is $r = 0.25$ nm, and I_{Ph} is the moment of inertia of the phenyl group for rotation around the double bond, $I_{\mathrm{Ph}} \approx m_2 r^2$, with $m_2 = 1.3 \cdot 10^{-22}$ g. The value of c_1 depends on the boundary condition. We use $c_1 = 4\pi$ for pure slip. The Stokes–Einstein relation is used to obtain β in terms of the self-diffusion coefficient of the solvent. As experimental diffusion and viscosity data on ethane and also propane[46,63] show that the ratio $Dn\sigma_1/k_B T = c_2$ is not constant with pressure, we use appropriately interpolated values for c_2.

The curves in Fig. 2 are the result of modeling the dependence of the rate coefficient on D^{-1} in liquid ethane, propane, and *n*-butane at room temperature with ω_B as a fit parameter. We used the energy barrier $E_{0,\mathrm{cl}}$ = 850 cm^{-1} given above, assuming that its value in propane will be approximately the same as in ethane and *n*-butane. The exact value

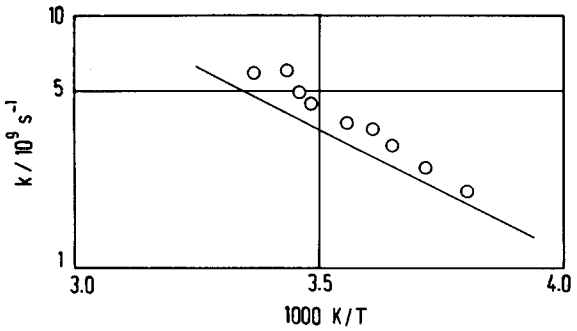

FIG. 9. Temperature dependence of DPB photoisomerization rate coefficients in liquid ethane below room temperature. (O: measurements from Courtney and Fleming[8]; solid line: model calculation from this work, see text.)

of K_{cl} is of no importance at these densities. In Figs. 9 and 10 we compare the temperature dependence of the rate coefficient predicted by our expression with the results obtained by Courtney and Fleming[8] in liquid ethane and propane at low temperatures. We used the parameter values obtained from the fit to our pressure dependent data. In ethane the model underestimates the rate coefficients by a factor of 1.3 on average, in propane it overestimates them by the same amount. The experimental temperature coefficient is about 20% higher than the prediction in both cases. In view of the limitations of the model and the uncertainties of the parameter values, however, this can be considered as good agreement with experiment.

So far the photoisomerization rate coefficient of DPB in liquid alkanes, therefore, appears consistent with the simple Kramers–Smoluchowski equation. In each of the solvents one observes proportionality between D and k. Changing the size of the solvent molecule, however, causes a shift of the turnover point into diffusion control along the D^{-1} axis, whereas the slope of the curve in the Kramers–Smoluchowski range does not change. This shift cannot be understood, if one only considers variations in solvent transport properties such as frequency dependent friction. There is also no reason to attribute these shifts to failures of the Stokes–Einstein relation, since it appears to be valid for each individual solvent. The deviation from the prediction of the simple Kramers–Smoluchowski expression observed for DPB in compressed liquid *n*-octane[6] and other high-viscosity solvents,[6,48] therefore, seems to be restricted to a regime of higher viscosities and does not have any influence on the rate coefficients in the "turnover" region we are discussing here.

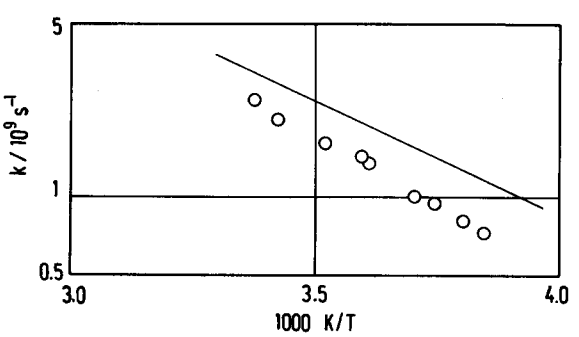

FIG. 10. Temperature dependence of DPB photoisomerization rate coefficients in liquid propane below room temperature. (O: measurements from Courtney and Fleming[8]; solid line: model calculation from this work, see text.)

The most plausible explanation of the observed shifts of the $k(D^{-1})$ curves along the D^{-1} axis appears to be again a cluster- or solvent-induced modification of the potential energy surface. Whereas modifications of the barrier height were considered in Sec. IV B, we now also suggest modifications of the imaginary barrier frequency ω_B. The curves in Fig. 2, for the three small alkane solvents at room temperature, were fitted with $\omega_B = 5\cdot10^{11}$, $6.5\cdot10^{11}$, and 2.10^{12} sec^{-1} for ethane, propane, and *n*-butane, respectively. For higher *n*-alkanes, ω_B seems to remain constant at a value close to that for propane. The very low value of ω_B compared to the double bond torsional mode frequency, which has been noted before for both stilbene[16] and DPB[6] in connection with the observation of an "anomalous" viscosity dependence of the rate coefficient in a series of different solvents, would indicate a very flat barrier to rotation around one of the double bonds. This is in agreement with our MNDO calculations for stilbene.[27] Apparently, the concept of a reaction being governed by a single torsional mode of the molecule is not sufficient here.[64] Additional experimental evidence for the importance of other coordinates, specifically phenyl ring rotation, comes from the observation of fast structural relaxation processes prior to twist around the double bond in picosecond experiments on DPB at low temperatures.[9] In view of MNDO calculations,[65] this was interpreted as a manifestation of phenyl ring rotation. The calculations showed that there is a marked dependence of the S_1 energy on the phenyl ring twist angle, and that the equilibrium configurations of ground and lowest excited state show a different angle, the molecule being more planar in the excited B_u^- state. This had been suggested before[66] following comparative spectroscopic studies of DPB and an analogous "stiff" compound, and was also concluded from recent time resolved UV resonance Raman experiments.[67] The change of the state ordering of the lowest ^1A_g and ^1B_u excited states of DPB on going from the dilute gas to the liquid phase is probably also reflecting the difference in the equilibrium phenyl ring rotation angle.[7,9,43] If the phenyl ring equilibrium conformation in both ground and excited states is affected by the environment, for instance by clustering with solvent molecules, one could imagine a substantial relative shift of states causing a change of the height and the shape of the barrier as well.

D. Multidimensional barrier effects in the Kramers–Smoluchowski range

Having fixed the parameters k_∞ and ω_B, we now compare our measurements of the temperature dependence of k in the Kramers–Smoluchowski range with the corresponding model predictions. Inspection of Fig. 6 indicates that the temperature dependence in this range is much stronger than

in the transition range to k_∞. The dependence by far exceeds that of the additional contribution from the temperature dependence of the friction (see Fig. 7). In order to accommodate for this effect, one either may try to use temperature dependent apparent barrier heights or temperature dependent apparent imaginary barrier frequencies. The dashed curves in Fig. 5 demonstrate the attempt to choose the former possibility for three isotherms in ethane. Keeping a fixed value of $\omega_B = 5\cdot10^{11}\ \mathrm{sec}^{-1}$, barrier heights of $E_{0,\mathrm{cl}}$ (295 K) $= 850\ \mathrm{cm}^{-1}$, $E_{0,\mathrm{cl}}$ (337 K) $= 700\ \mathrm{cm}^{-1}$, and $E_{0,\mathrm{cl}}$ (370 K) $= 650\ \mathrm{cm}^{-1}$ had to be chosen. This representation, however, appears unsatisfactory, since the shape of the curve at 370 K does not correspond closely to the observed $k(D^{-1})$ dependence of the rate coefficients. The same applies to the data shown in Fig. 6. Better agreement is found by choosing temperature dependent apparent barrier frequencies. The solid curves in Fig. 5 show the results obtained by keeping $E_{0,\mathrm{cl}} = 850\ \mathrm{cm}^{-1}$ fixed and using for ethane the barrier frequencies $\omega_B(295\ \mathrm{K}) = 5\cdot10^{11}\ \mathrm{sec}^{-1}$, $\omega_B(337\ \mathrm{K}) = 1.1\cdot10^{12}\ \mathrm{sec}^{-1}$, and $\omega_B(370\ \mathrm{K}) = 1.5\cdot10^{12}\ \mathrm{sec}^{-1}$. The curves in Fig. 6 show the corresponding fits to the propane isotherms with $E_{0,\mathrm{cl}} = 850\ \mathrm{cm}^{-1}$, $\omega_B(298\ \mathrm{K}) = 6.5\cdot10^{11}\ \mathrm{sec}^{-1}$, and $\omega_B(390\ \mathrm{K}) = 2.5\cdot10^{12}\ \mathrm{sec}^{-1}$. For CO_2, $E_{0,\mathrm{cl}} = 900\ \mathrm{cm}^{-1}$ and $\omega_B(350\ \mathrm{K}) = 3\cdot10^{13}\ \mathrm{sec}^{-1}$ gave the best fit.

The increase in the temperature coefficient of k in the Kramers–Smoluchowski range beyond the prediction of a model with temperature independent effective barrier height or imaginary barrier frequency is very pronounced. We illustrate this again in Fig. 11, in which a "reduced rate coefficient" k_{red} is shown, being defined by

$$k_{\mathrm{red}}(T) = k(T)\cdot[1+\beta(T)/\omega_B(295\ \mathrm{K})]. \tag{14}$$

For the one-dimensional Kramers–Smoluchowski model of Eqs. (8) and (12)—neglecting the k_0 term—$k_{\mathrm{red}}(T)$ should be equal to $k_\infty(T)$, which is also shown in Fig. 11 for comparison. While the low-temperature values of $k_{\mathrm{red}}(T)$ roughly agree with $k_\infty(T)$, at temperatures above the critical temperature T_c of ethane significant deviations appear. For ethane they can be empirically represented by

$$\omega_B(T>T_c) \approx \omega_B(295\ \mathrm{K}) \cdot \exp[2.03\cdot10^3\ \mathrm{K}\cdot(1/T_c - 1/T)], \tag{15}$$

as shown by the small points in Fig. 11. In the following we propose possible explanations for this observation.

At first, we inspect the consequences of barrier anharmonicity in a one-dimensional Kramers–Smoluchowski treatment. In the high-damping limit the rate coefficient k is given by[68–70]

$$k \approx \frac{k_\infty}{\beta}\sqrt{\frac{2\pi k_B T}{I}}\cdot\left[\int_{-\infty}^{\infty}\exp\left(\frac{[(V(r)-E_0]}{k_B T}\right)\cdot dr\right]^{-1}. \tag{16}$$

Using a barrier shape of

$$V(r) = E_0 - A\cdot(r-r_0)^{2n}, \tag{17}$$

this leads to

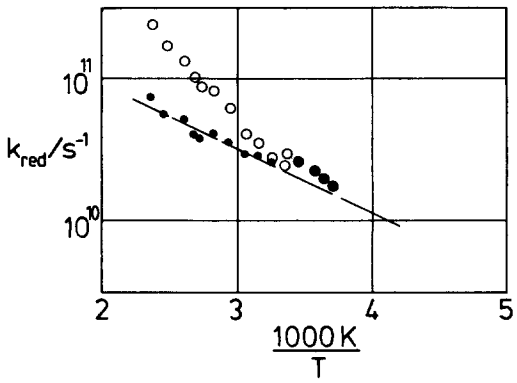

FIG. 11. Reduced rate coefficients k_{red} from Eq. (14) reflecting temperature dependent effective barrier frequencies, see Eq. (23). (Experimental points from Fig. 7; dashed line: Kramers–Smoluchowski representation with $E_{0,\mathrm{cl}} = 850\ \mathrm{cm}^{-1}$ and $\omega_B(295\ \mathrm{K}) = 5.0\cdot10^{11}\ \mathrm{sec}^{-1}$. Small points: $k_{red}(T)$ with temperature dependent $\omega_B(T)$ from Eq. (15).)

$$k \approx \frac{k_\infty}{\beta}\cdot\sqrt{\frac{2\pi k_B T}{I}}\cdot\left(\frac{n}{\Gamma(1/2n)}\cdot(A/k_B T)^{1/2n}\right). \tag{18}$$

For $n = 1$, the result of Eq. (12) with a temperature independent imaginary barrier frequency is recovered. For a completely flat barrier, i.e., $n\to\infty$, an apparent imaginary barrier frequency is obtained, which increases as

$$\omega_B \propto \sqrt{T}. \tag{19}$$

While this consequence of anharmonicity of a very flat barrier may contribute to our observations, the effect is by far too small to account for the temperature dependence shown in Fig. 11.

Next we inspect the consequences of multidimensional barrier shapes. Our MNDO calculations for stilbene[27] suggest that the flatness of the barrier decreases, when at least one coordinate "perpendicular" to the reaction coordinate is excited. (In stilbene this was the orientation of the phenyl rings relative to the plane of the ethylene bridge.) Including an increase of the barrier frequency ω_B with excitation of at least one further coordinate "2" in the form

$$\omega_B(E_2) \approx \omega_{B0}\cdot(E_2/a)^b, \tag{20}$$

we calculate k to a first approximation by averaging of Eq. (12) over a thermal distribution of activated complex states. Via

$$k \approx \frac{\omega_{B0}}{\beta}\cdot k_\infty\cdot\int_0^\infty\left(\frac{E_2}{a}\right)^b\cdot\exp\left(\frac{-E_2}{k_B T}\right)\cdot\frac{dE_2}{k_B T} \tag{21}$$

we obtain

$$k \approx (\omega_{B0}/\beta)\cdot k_\infty\cdot(k_B T/a)^b\cdot\Gamma(b+1). \tag{22}$$

More sophisticated treatments appear premature as long as the details of the potential are not better characterized. In particular, the dependence of ω_B on several other coordinates may result in multiplicative effects. According to Eqs. (20) and (22), strong energy dependences of ω_B result in strong temperature dependences of the apparent imaginary barrier frequency:

$$\omega_B(T) \approx \omega_{B0} \cdot (k_B T/a)^b \cdot \Gamma(b+1). \quad (23)$$

In the present case, a value of $b \approx 4.9$ would reproduce the fitted values of $\omega_B(T)$. As stated before, $b = \Sigma b_i$ may include the contributions from several coordinates i "perpendicular" to the reaction coordinate.

IV. CONCLUSIONS

In the present paper we have demonstrated cluster- (or solvent-) induced modifications of the potential energy surface of the photoisomerization of DPB. Apart from this, the multidimensionality of this surface manifests itself in various ways. Our experiments suggest that such effects can also be identified via the temperature dependence of the rate coefficients in the Kramers–Smoluchowski range. At constant temperature, the Kramers–Smoluchowski representation works well for the low-viscosity solvents considered in the present work. In order to prove the suggestions given here, detailed quantum-chemical calculations of the potential energy surface of the free and the clustered molecule appear indispensible.

ACKNOWLEDGMENT

Financial support of this work by the Deutsche Forschungsgemeinschaft (Sonderforschungsbereich 93 "Photochemie mit Lasern") is gratefully acknowledged.

[1] J. F. Shepanski, B. W. Keelan, and A. H. Zewail, Chem. Phys. Lett. **103**, 9 (1983).
[2] A. Amirav, M. Sonnenschein, and J. Jortner, Chem. Phys. **102**, 305 (1986).
[3] J. S. Horwitz, B. E. Kohler, and T. A. Spiglanin, J. Chem. Phys. **83**, 2186 (1985).
[4] L. A. Heimbrook, B. E. Kohler, and T. A. Spiglanin, Proc. Natl. Acad. Sci. USA **80**, 4580 (1983).
[5] J. Troe, A. Amirav, and J. Jortner, Chem. Phys. Lett. **115**, 245 (1985).
[6] S. P. Velsko and G. R. Fleming, J. Chem. Phys. **76**, 3553 (1982).
[7] G. Maneke, J. Schroeder, J. Troe, and F. Voβ, Springer Proc. Phys. **4**, 156 (1985).
[8] S. H. Courtney and G. R. Fleming, Chem. Phys. Lett. **103**, 443 (1984).
[9] C. Rulliere, A. Declemy, and Ph. Kottis, Laser Chem. **5**, 185 (1985).
[10] J. Schroeder and J. Troe, Annu. Rev. Phys. Chem. **38**, 163 (1987).
[11] J. A. Syage, W. R. Lambert, P. M. Felker, A. H. Zewail, and R. M. Hochstrasser, Chem. Phys. Lett. **88**, 266 (1982).
[12] A. Amirav and J. Jortner, Chem. Phys. Lett. **95**, 295 (1983).
[13] T. J. Majors, U. Even, and J. Jortner, J. Chem. Phys. **81**, 2330 (1984).
[14] B. I. Greene, R. M. Hochstrasser, and R. B. Weisman, J. Chem. Phys. **71**, 544 (1979); Chem. Phys. **48**, 289 (1980).
[15] L. A. Brey, G. B. Schuster, and H. G. Drickamer, J. Am. Chem. Soc. **101**, 129 (1979).
[16] G. Rothenberger, D. K. Negus, and R. M. Hochstrasser, J. Chem. Phys. **79**, 5360 (1983).
[17] V. Sundström and T. Gillbro, Chem. Phys. Lett. **109**, 538 (1984); Ber. Bunsenges. Phys. Chem. **89**, 222 (1985).
[18] S. H. Courtney and G. R. Fleming, J. Chem. Phys. **83**, 215 (1985).
[19] G. Maneke, J. Schroeder, J. Troe, and F. Voβ, Ber. Bunsenges. Phys. Chem. **89**, 896 (1985).
[20] M. Lee, G. R. Holtom, and R. M. Hochstrasser, Chem. Phys. Lett. **118**, 359 (1985).
[21] M. Lee, A. J. Bain, P. J. McCarthy, C. H. Han, J. N. Haseltine, A. B. Smith III, and R. M. Hochstrasser, J. Chem. Phys. **85**, 4341 (1986).
[22] S. H. Courtney, S. K. Kim, S. Canonica, and G. R. Fleming, J. Chem. Soc. Faraday **82**, 2065 (1986); S. K. Kim and G. R. Fleming, J. Phys. Chem. **92**, 2168 (1988).
[23] J. Troe, Chem. Phys. Lett. **114**, 241 (1985).
[24] J. A. Syage, P. M. Felker, and A. H. Zewail, J. Chem. Phys. **81**, 4706 (1984).
[25] J. Schroeder and J. Troe, J. Phys. Chem. **90**, 4215 (1986).
[26] J. Troe, J. Phys. Chem. **90**, 357 (1986).
[27] J. Troe and K.-M. Weitzel, J. Chem. Phys. **88**, 7030 (1988).
[28] J. Troe, Habilitationsschrift, Göttingen, 1967.
[29] J. Troe in *High Pressure Chemistry*, edited by H. Kelm (Reidel, Dordrecht, 1978), p. 489.
[30] J. Troe in *Physical Chemistry. An Advanced Treatise*, edited by W. Jost (Academic, New York, 1975), Vol. VIB, p. 835.
[31] For recent reviews see J. T. Hynes, in *The Theory of Chemical Reaction Dynamics*, edited by M. Baer (Chemical Rubber, Boca Raton, 1985), Vol. 4, p. 171; J. T. Hynes, Annu. Rev. Phys. Chem. **36**, 573 (1985); J. Stat. Phys. **42**, 149 (1986); G. H. Weiss, J. Stat. Phys. **42**, 3 (1986); P. Hänggi, J. Stat. Phys. **42**, 105 (1986); F. Marchesoni, Adv. Chem. Phys. **63**, 603 (1986); D. Chandler, J. Stat. Phys. **42**, 49 (1986); J. A. Montgomery, Jr., D. Chandler, and B. J. Berne, J. Chem. Phys. **70**, 4056 (1979); J. E. Straub, M. Borkovec, and B. J. Berne, J. Chem. Phys. **84**, 1788 (1986); J. E. Straub and B. J. Berne, J. Chem. Phys. **85**, 2999 (1986); R. E. Cline, Jr. and P. G. Wolynes, J. Chem. Phys. **86**, 3836 (1987); R. O. Rosenberg, B. J. Berne, and D. Chandler, Chem. Phys. Lett. **75**, 162 (1980); D. Statman and G. W. Robinson, J. Chem. Phys. **83**, 655 (1985); A. Nitzan, J. Chem. Phys. **86**, 2734 (1987); J. E. Straub and B. J. Berne, J. Chem. Phys. **87**, 6111 (1987); M. Borkovec and B. J. Berne, J. Chem. Phys. **82**, 794 (1985); A. Nitzan, J. Chem. Phys. **82**, 1614 (1985).
[32] R. Landauer and J. A. Swanson, Phys. Rev. **121**, 1668 (1961).
[33] J. S. Langer, Ann. Phys. **54**, 258 (1969).
[34] Z. Schuss and B. J. Matkowsky, SIAM J. Appl. Math. **35**, 604 (1979).
[35] H. Weidenmüller and Z. Jing-Shang, J. Stat. Phys. **34**, 191 (1984).
[36] M. M. Klosek-Dygas, B. M. Hoffmann, B. J. Matkowsky, A. Nitzan, M. A. Ratner, and Z. Schuss, J. Chem. Phys. **90**, 1141 (1989).
[37] A. M. Berezhkovskii, L. M. Berezhkovskii, and V. Yu. Zitzerman, Chem. Phys. **130**, 55 (1989); A. M. Berezhkovskii and V. Yu. Zitzerman, Chem. Phys. Lett. **158**, 369 (1989).
[38] S. Lee and M. Karplus, J. Phys. Chem. **92**, 1075 (1988).
[39] N. Agmon and R. Kosloff, J. Phys. Chem. **91**, 1988 (1987).
[40] B. J. Matkowsky, A. Nitzan, and Z. Schuss, J. Chem. Phys. **88**, 4765 (1988); **90**, 1292 (1989).
[41] R. S. Larson and M. D. Kostin, J. Chem. Phys. **77**, 5017 (1982).
[42] H. E. Lessing and A. von Jena, Chem. Phys. Lett. **42**, 213 (1976).
[43] R. A. Goldbeck, A. J. Twarowski, E. L. Russell, J. K. Rice, R. R. Birge, E. Switkes, and D. S. Kliger, J. Chem. Phys. **77**, 3319 (1982).
[44] R. Mehnert, W. Helmstreit, J. Bös, and O. Brede, Radiochem. Radioanal. Lett. **30**, 389 (1977); T. Shida and W. H. Hamill, J. Chem. Phys. **44**, 4372 (1966).
[45] J. Schroeder and J. Troe, Chem. Phys. Lett. **116**, 453 (1985).
[46] C. G. Wade and J. S. Waugh, J. Chem. Phys. **43**, 3555 (1965).
[47] B. I. Lee and M. G. Kesler, A. I. Chem. Eng. J. **21**, 510 (1975); J. O. Hirschfelder, C. F. Curtiss, and R. B. Bird, "Molecular Theory of Gases and Liquids" (J. Wiley, New York, 1954).
[48] J. Schroeder, D. Schwarzer, J. Troe, and F. Voβ (to be published).
[49] K. W. Hausser, R. Kuhn, and G. Seitz, Z. Physikal, Chem. B **29**, 391 (1935).
[50] S. L. Frye, C. R. Yonker, D. R. Kalkwarf, and R. D. Smith, ACS Symposium Ser. **329**, 27 (1987).
[51] J. Troe, J. Phys. Chem. **88**, 4375 (1984).
[52] B. M. Pierce and R. R. Birge, J. Chem. Phys. **86**, 2651 (1982).
[53] J. Troe, J. Chem. Phys. **66**, 4745, 4758 (1977).
[54] J. Troe, J. Phys. Chem. **83**, 114 (1979).
[55] J. Troe, J. Phys. Chem. **87**, 1800 (1983).
[56] B. Otto, J. Schroeder, and J. Troe, J. Chem. Phys. **81**, 202 (1984).
[57] S. H. Courtney, G. R. Fleming, L. R. Khundkar, and A. H. Zewail, J. Chem. Phys. **80**, 4559 (1984).
[58] S. H. Courtney, M. W. Balk, L. A. Philips, S. P. Webb, D. Yang, D. H. Levy, and G. R. Fleming, J. Chem. Phys. **89**, 6697 (1988).
[59] L. R. Khundkar, R. A. Marcus, and A. H. Zewail, J. Phys. Chem. **87**, 2473 (1983).
[60] S. Nordholm, Chem. Phys. **137**, 109 (1989).
[61] J. S. McCaskill and R. G. Gilbert, Chem. Phys. **44**, 389 (1979).
[62] R. C. Reid, J. M. Prausnitz, and T. K. Sherwood, *The Properties of Gases and Liquids* (McGraw-Hill, New York, 1977).
[63] R. C. Robinson and W. E. Stewart, I&EC Fundam. **7**, 91 (1968); P. M. Holland, H. J. M. Hanley, K. E. Gubbins, and J. M. Haile, J. Phys. Chem. Ref. Data **8**, 559 (1979); H. J. M. Hanley, K. E. Gubbins, and S. Murad, J. Phys. Chem. Ref. Data **6**, 1167 (1977); **10**, 799 (1981).
[64] E. Pollak, J. Chem. Phys. **86**, 3944 (1987).
[65] C. Rulliere, A. Declemy, Ph. Kottis, and L. Ducasse, Chem. Phys. Lett.

117, 583 (1985).
[66]W. A. Yee, J. S. Horowitz, R. A. Goldbeck, C. M. Einterz, and D. S. Kliger, J. Phys. Chem. **87**, 380 (1983).
[67]R. L. Gustafson, J. F. Palmer, and D. M. Roberts, Chem. Phys. Lett. **127**, 505 (1986).
[68]M. v. Smoluchowski, Phys. Z. **17**, 557,585 (1916).
[69]H. A. Kramers, Physica **7**, 284 (1940).
[70]S. Chandrasekhar, Rev. Mod. Phys. **15**, 1 (1943).
[71]B. A. Younglove and J. F. Ely, J. Phys. Chem. Ref. Data **16**, 577 (1987).
[72]S. E. Babb, Jr., and S. L. Robertson, J. Chem. Phys. **53**, 1097 (1970).
[73]S. E. Babb, Jr., and G. J. Scott, J. Chem. Phys. **40**, 3666 (1964).
[74]A. Michels, A. Botzen, and W. Schuurman, Physica **23**, 95 (1957); W. Kurin and I. F. Golubev, Teploenergetika **21**, 84 (1974).
[75]A. Boushehri, J. Bziwski, J. Kestin, and E. A. Mason, J. Phys. Chem. Ref. Data **16**, 445 (1987).
[76]J. H. Dymond, Chem. Phys. **17**, 101 (1976).
[77]Landolt-Börnstein, *Zahlenwerte und Funktionen*, 6.Auflage, Band II/1 (Springer, Heidelberg, 1971).
[78]D. S. Viswanath and G. Natarajan, *Viscosity of Liquids* (Hemishere, New York, 1989).
[79]*Handbook of Chemistry and Physics* (Chemical Rubber, Boca Raton, 1973).
[80]F. Bachl and H.-D. Lüdemann, Z. Naturforsch. **41a**, 963 (1986).